THE JOURNAL OF PROSTHETIC DENTISTRY

RESEARCH AND EDUCATION

Effects of the internal contact surfaces of dental implants on screw loosening: A 3-dimensional finite element analysis

Abdulrahman Al-sanea, BS, MSc, MSc,[a] Serkan Aktas, BS, MSc, PhD,[b] Talip Celik, BS, MSc, PhD,[c] and Yasin Kisioglu, BS, MSc, PhD[d]

ABSTRACT

Statement of problem. The effects of the internal contact surfaces of dental implants on screw loosening have yet to be investigated.

Purpose. The purpose of this 3-dimensional finite element analysis (FEA) study was to evaluate and compare the mechanical effects of the abutment implant angle (θ), the abutment screw head diameter (D), and the abutment screw length (L) on screw loosening.

Material and methods. A total of 27 models presenting various mechanical scenarios were built by using combinations of 3 different θ (30 degrees, 45 degrees, and 60 degrees), D (2.65 mm, 2.75 mm, and 2.85 mm), and L (4 mm, 5 mm, and 6 mm). In FEA, a static test with a 200-N force inclined 30 degrees in the implant axial direction was applied to the upper surface of the abutment to evaluate and compare the maximum von Mises stresses of the implant components and the maximum total deformation in all models. In addition, modal analysis was applied to identify the natural frequencies in all models under free (unforced) vibration, and a Kruskal-Wallis statistical test (α=.05) was performed, followed by multiple pairwise comparisons by using the Dunn test.

Results. The Kruskal-Wallis test found a significant influence of the θ on implant stress, total deformation, and natural frequency (*P*<.001). For example, increasing the θ from 30 degrees to 45 degrees and 60 degrees can considerably reduce the model's natural frequencies to 18% and 26%, respectively. Similarly, the test underscored the significant impact of the D on both abutment screw stress and abutment stress (*P*=.010 and *P*=.002, respectively). However, the L appeared to have no significant effect on any of the dependent variables (*P*>.05).

Conclusions. The θ and the D significantly influenced the stresses of dental implant components, total deformation, and natural frequency of the model, which may impact the mechanical stability of the screw joint. However, the L does not appear to affect these values significantly. (J Prosthet Dent 2023;130:603.e1-e11)

Abutment screw loosening is a common complication with implant-supported prostheses, with the incidence of screw loosening varying widely across different conditions and patient groups.[1–6] For instance, Goodacre et al[7] reported that abutment screw loosening occurred in 6% of 6256 implants, even reaching up to 45% in single crowns. This high frequency underscores the persistent challenge screw loosening poses to dental implant manufacturers and practitioners and the need for further research.

The different conditions included screw length,[8–10] implant diameter,[11] contamination during the treatment process,[12] implant-abutment connection designs,[13,14] lateral forces,[11,15] and torque values,[16–18] among others.[2,19–43] While these studies have highlighted some aspects of screw loosening, a significant knowledge gap remains. Specifically, the internal contact surfaces of dental implants, a potentially crucial factor in screw loosening, have been largely overlooked.

The present research examined the influence of internal contact surfaces, specifically the abutment implant angle (θ), the abutment screw head diameter (D), and the abutment screw length (L), on screw loosening in dental

Supported by the Scientific Research Projects Coordination Unit of Kocaeli University (project FYL-2022-3028), Uzunciftlik Nuh Cimento Vocational High School, and Biomechanics Lab in the Biomedical Engineering Department at Kocaeli University, Kocaeli, Turkey.
The authors declare that there are no conflicts of interest to disclose.
[a]Graduate student, Department of Biomedical Engineering, Biomechanics Lab, Kocaeli University, Kocaeli, Turkey.
[b]Lecturer, Uzunciftlik Nuh Cimento Vocational High School, Kocaeli University, Kocaeli, Turkey.
[c]Associate Professor, Department of Biomedical Engineering, Biomechanics Lab, Kocaeli University, Kocaeli, Turkey.
[d]Full Professor, Department of Biomedical Engineering, Biomechanics Lab, Kocaeli University, Kocaeli, Turkey.

Clinical Implications

The incidence of abutment screw loosening can be influenced by modifications that increase the contact area within dental implants. An increase in the abutment screw head diameter and a decrease in the abutment implant angle may improve the screw joint stability, contributing to solving one of the most common issues encountered by dental implant manufacturers.

implants. The authors are unaware of previous studies on the collective effect of these parameters on screw loosening. Whether these 3 parameters significantly influence screw loosening remains unclear, and if so, which has the most substantial impact. Finite element analysis (FEA) and various statistical tests were conducted to determine the interplay between these parameters and their collective influence on the mechanical stability of the screw joint.

FEA has been widely adopted in biomedical engineering applications and has been used in many studies to evaluate abutment screw loosening.[8,21,22,44–48] Chen et al[44] indicated that some FEA studies directly linked the increase in maximum von Mises stresses in the abutment screw with screw loosening. Therefore, in the present study, the maximum von Mises stress and the maximum total deformation of dental implant components, particularly the abutment screw and implant, were used to evaluate and compare screw loosening in all models. Additionally, the natural frequencies of the vibrational modes of the model were assessed by using modal analysis, an approach that is particularly useful for assessing the dynamic behavior of a system.[49]

The null hypotheses were that the θ, D, and L would not have a significant effect on the stresses of dental implant components, total deformation, or natural frequency of dental implant design and that they would not influence the mechanical stability of the screw joint and the probability of screw loosening in dental implants.

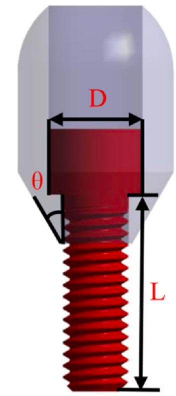

Figure 1. Implant design parameters investigated. θ, abutment implant angle; D, abutment screw head diameter; L, abutment screw length.

Table 1. Combinations of abutment implant angle (θ), abutment screw head diameter (D), and abutment screw length (L) with model nodes and element numbers used

Abutment Implant Angle (θ) (degrees)	Screw Head Diameter (D) (mm)	Screw Length (L) (mm)	Node Number	Element Number
30	2.65	4	253255	170557
		5	291182	196586
		6	327407	221391
	2.75	4	264181	178301
		5	301131	203631
		6	338699	229433
	2.85	4	274004	185560
		5	311451	211289
		6	348092	236376
45	2.65	4	253963	171066
		5	291401	196781
		6	327816	221694
	2.75	4	264489	178585
		5	301616	204059
		6	338834	229561
	2.85	4	274593	186039
		5	311626	211438
		6	348388	236586
60	2.65	4	254049	171158
		5	291375	196767
		6	304511	207918
	2.75	4	268980	181205
		5	301196	203740
		6	338507	229342
	2.85	4	274370	185926
		5	311683	211525
		6	347807	236199

MATERIAL AND METHODS

Both static and modal analyses were used to evaluate and compare the stability of 27 models through the evolution of the maximum von Mises stresses for the implant components, maximum total deformation, and natural frequencies. The static analysis provided insight into the stress distribution and deformation under a 200-N load, whereas modal analysis helped in understanding the dynamic response and stability of the dental implant system under unforced vibration. Combining these 2 approaches provided a more thorough evaluation of the factors affecting screw loosening in dental implants.

The implant, the abutment, and the abutment screw were analyzed with the parameters illustrated in Figure 1. Three L (4 mm, 5 mm, and 6 mm), 3 D (2.65 mm, 2.75 mm, and 2.85 mm), and 3 θ (30 degrees, 45 degrees, and 60 degrees) were evaluated, with a total of 27 combinations (Table 1, Fig. 2).

Solid components of the 27 implants were constructed and assembled by using a 3-dimensional (3D) computer-aided design (CAD) software program (SolidWorks version 2020; Dassault Systèmes SolidWorks Corp) and exported into a CAD modeling software program (ANSYS version 21; ANSYS, Inc) for analysis (Fig. 2). According to the mesh convergence,

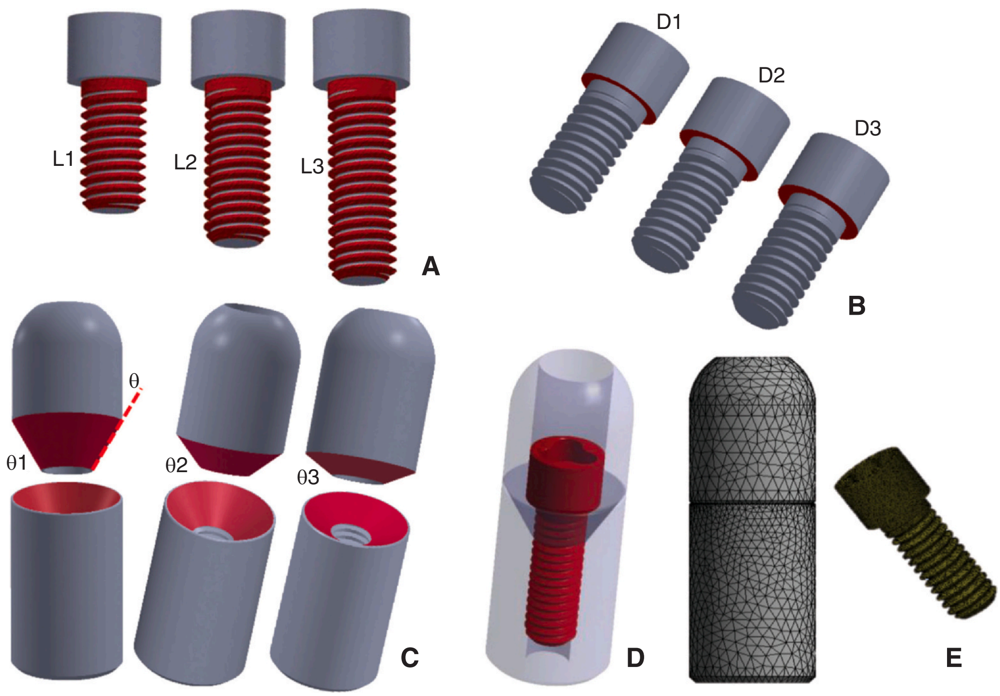

Figure 2. Three-dimensional computer-aided design models used with different parameters. A, Abutment screw lengths: 4 mm (L1), 5 mm (L2), and 6 mm (L3). B, Abutment screw head diameters: 2.65 mm (D1), 2.75 mm (D2), 2.85 mm (D3). C, Abutment implant angles: 30 degrees (θ1), 45 degrees (θ2), and 60 degrees (θ3). D, Assembled model. E, Mesh model.

Table 2. Measurements and preload value for model

Parameters	Value
T (Nmm)	250
P (mm)	0.35
μ_t	0.2
μ_n	0.2
d_2 (mm)	1.78
d_n (mm)	2
β (deg)	30
F (N)	542

the screw element size was selected as 0.1 mm, and the element size of other components was 0.25 mm. The mesh of the total model is shown in Figure 2E. After the 27 finite element (FE) mesh models had been developed, friction was assumed between all implant components, with a friction coefficient of 0.2.[50]

A tightening torque of 25 Ncm was applied to the screw to simulate preload, calculated by substituting the values of the abutment screw design parameters (Table 2, Fig. 3) in the torque euqation (Eq. [1]). A torque of 25 Ncm with a coefficient of friction of 0.2 assumed for all screw threads and screw head resulted in a preload of 542 N, which was transformed along the interface between the surface of the threads of the abutment screw and the surface of the internal threads of the screw channel (Fig. 4A).

Figure 3B illustrates the interface between the screw and the screw channel in the implant design. The screw channel was a threaded, cylindrical hole within the implant body, whereas the abutment screw had a matching threaded outer surface.

A 200-N force inclined 30 degrees in the axial direction was applied to the upper surface of the abutment (Fig. 4B) to simulate the maximum masticatory load in the posterior area.[50,51] All sides of the external surface of the implant were fixed as boundary conditions before the simulation was carried out (Fig. 4C). The mechanical properties of the materials, including the Poisson ratio and elastic modulus, were standardized, and all materials were assumed to be isotropic, homogeneous, and linearly elastic (Table 3).[50,52–54]

The torque equation was used to calculate the screw preload applied in all models:

$$T = \frac{F}{2}\left[\frac{p}{\pi} + \frac{\mu_t d_2}{\cos\beta} + d_n\mu_n\right] \quad (1)$$

By solving for F

$$F = \frac{2T}{\left[\frac{p}{\pi} + \frac{\mu_t d_2}{\cos\beta} + d_n\mu_n\right]} \quad (2)$$

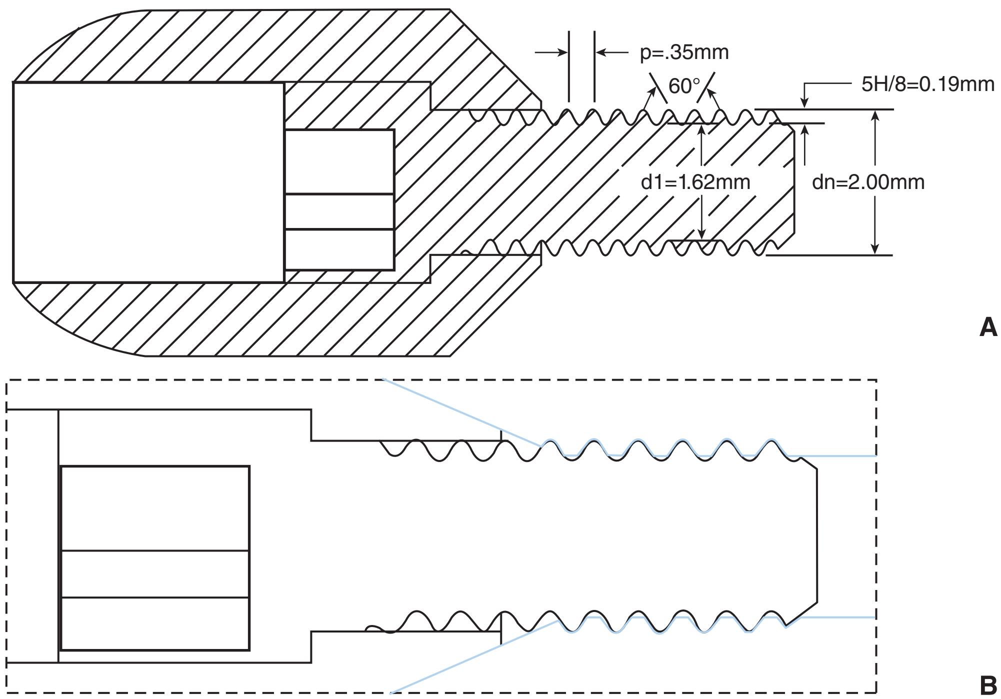

Figure 3. A, Abutment screw design parameters values used. B, Interface between abutment screw and screw channel.

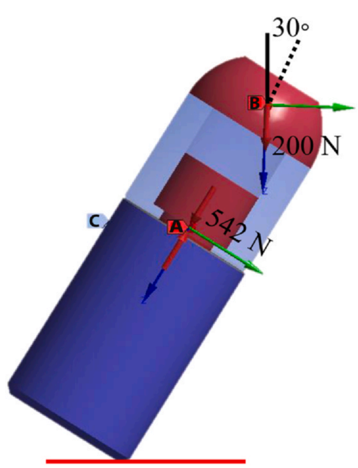

Figure 4. Boundary conditions used. A, Screw preload 542 N. B, Load applied to upper surface of abutment 200 N. C, Fixed support (external surface of implant).

where, T (Nmm)=tightening torque, P (mm)=thread pitch, μ_t=coefficient of friction for the threads, μ_n=coefficient of friction for the screw head, d_2 (mm)=pitch diameter of the thread, d_n (mm)=major diameter of the thread, β (deg)=flank angle, and F (N)=screw preload.

By substituting the values of the abutment screw design parameters from Table 2 into Equation (2)

$$F = \frac{2*250}{\left[\frac{0.35}{\pi} + \frac{0.2*1.78}{\cos 30} + 2*0.2\right]} \cong 542N$$

The natural frequencies of the 27 models were identified under free vibration by using modal analysis in the ANSYS software program. Free vibration referred to the oscillatory motion of the dental implant in the absence of external forces.

To determine whether there were significant differences between factor groups, a nonparametric Kruskal-Wallis statistical test was used because of the nonnormal distribution of some of the data, as determined by the Shapiro-Wilk normality test. After the Kruskal-Wallis test, multiple pairwise comparisons were conducted by using the Dunn test. Statistical analyses were performed by using a statistical software program (IBM SPSS Statistics, v29.0.1.0; IBM Corp) (α=.05).

RESULTS

The findings of the static test and modal analysis are presented in Table 4. Figure 5 illustrates stress distribution in implant components for 1 model. As shown in Table 5, the Kruskal-Wallis test revealed a significant influence of the θ on implant stress, total deformation, and natural frequency (P<.001). Furthermore, the Dunn test reported significant differences (P<.05) among all 3 group pairs (30 to 45, 30 to 60, and 45 to 60 degrees) for the same measured values, except for total deformation between the 45 and 60-degree group pair (P=.272) (Table 6).

The D significantly affected both abutment screw stress and abutment stress (P=.010 and P=.002, respectively)

Table 3. Material properties used in analysis

Components	Material	Elastic Modulus E (GPa)	Poisson Ratio υ	Yield Strength σ (MPa)
Abutment screw, abutment, implant	Titanium Alloy (Ti-6Al-4V)	110	0.35	860

Table 4. Maximum von Mises stress of implant components, total deformation, and natural frequency for all models

Abutment Angle (θ) (degrees)	Screw Head Diameter (D) (mm)	Screw Length (L) (mm)	Maximum von Mises Stress of Abutment Screw (MPa)	Maximum von Mises Stress of Abutment (MPa)	Maximum von Mises Stress of Implant (MPa)	Maximum Total Deformation of Model (mm)	Natural Frequency of Model (Mode 1) (Hz)
30	2.65	4	666.64	261.16	738.10	0.0075079	92098
30	2.65	5	697.32	259.64	711.80	0.0075121	92136
30	2.65	6	689.02	261.00	729.58	0.0075484	92085
30	2.75	4	693.21	240.12	566.33	0.0077083	92753
30	2.75	5	716.85	239.98	580.10	0.0076633	92772
30	2.75	6	721.58	239.64	728.03	0.0076963	92722
30	2.85	4	721.66	354.50	237.43	0.0085641	93138
30	2.85	5	680.09	197.50	605.19	0.0078479	93445
30	2.85	6	695.73	197.83	721.06	0.0078792	93401
45	2.65	4	703.45	264.28	1036.5	0.0089318	75180
45	2.65	5	675.11	263.13	956.87	0.0088812	75186
45	2.65	6	671.84	263.92	663.42	0.0089596	75418
45	2.75	4	702.49	243.25	1035.3	0.0091241	75864
45	2.75	5	926.25	284.46	823.28	0.0353830	75871
45	2.75	6	733.63	242.72	1584.9	0.0091323	75808
45	2.85	4	737.75	216.06	1280.1	0.0092667	76715
45	2.85	5	661.6	215.13	898.50	0.0091817	76727
45	2.85	6	712.38	215.37	1588.8	0.0093205	76662
60	2.65	4	660.99	267.31	482.28	0.0085860	67679
60	2.65	5	674.54	266.40	475.94	0.0086431	67709
60	2.65	6	707.54	270.53	443.77	0.0112000	65672
60	2.75	4	747.46	299.99	313.91	0.0092026	68463
60	2.75	5	691.57	239.66	476.16	0.0088097	68433
60	2.75	6	738.27	238.81	417.76	0.0087534	68417
60	2.85	4	724.89	213.18	470.46	0.0089609	69199
60	2.85	5	675.78	212.98	507.32	0.0090377	69218
60	2.85	6	722.25	212.90	471.25	0.0089451	69210

(Table 5). The Dunn test revealed significant differences in abutment screw stress between the group pair (2.65 to 2.75) mm and in abutment stress between the group pairs (2.65 to 2.85) mm, and (2.75 to 2.85) mm (Table 6). However, L had no significant effect on any of the dependent variables ($P>.05$) (Table 5).

The main effect of the maximum von Mises equivalent stress indicated that the implant stress was influenced by the θ. For example, the rate of change in implant stress was 76% and −28% when the θ increased from 30 degrees to 45 degrees and 60 degrees, respectively (Fig. 6A). Additionally, the maximum total deformation of the models significantly increased to 55% when the θ changed from 30 to 45 degrees ($P<.001$) and increased, but at a lesser rate of 17% when the angle changed from 30 to 60 degrees ($P=.002$) (Table 6, Fig. 6A). Furthermore, the main effect plot (Fig. 6A) reveals a decrease in natural frequency corresponding to an increase in the θ. Specifically, when the angle of the abutment implant increased from 30 degrees to 45

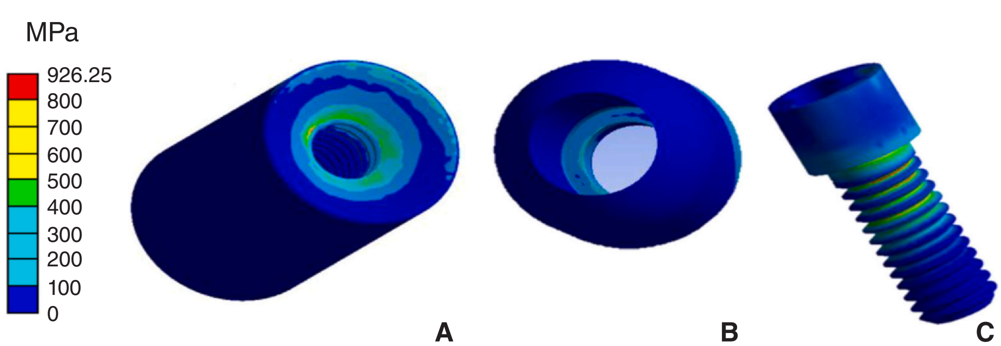

Figure 5. Stress distribution in one model. A, Implant. B, Abutment. C, Abutment screw.

Table 5. K independent Kruskal-Wallis test *P* values

Implant Design Parameter	Abutment Screw Stress	Abutment Stress	Implant Stress	Total Deformation	Natural Frequency
Abutment implant angle	.799	.852	<.001	<.001	<.001
Abutment screw head diameter	.010	.002	.952	.336	.276
Abutment screw length	.291	.291	.934	.917	.934

Table 6. Multiple pairwise comparisons by using Dunn test *P* values

Implant Design Parameter	Pairwise Comparisons	Abutment Screw Stress	Abutment Stress	Implant Stress	Total Deformation	Natural Frequency
Abutment implant angle (degrees)	Group 30-45			.018	<.001	.016
	Group 30-60			.043	.002	<.001
	Group 45-60			<.001	.272	.016
Abutment screw head diameter (mm)	Group 2.65-2.75	.003	.181			
	Group 2.65-2.85	.070	<.001			
	Group 2.75-2.85	.235	.033			

degrees and 60 degrees, the natural frequencies of the models decreased to 18% and 26%, respectively.

For the main effect of D, the maximum von Mises stress of the abutment screw increased to 9% when the diameter changed from 2.65 to 2.75 mm (*P*<.05) and increased to 3% when the diameter increased from 2.65 to 2.85 mm (Table 6, Fig. 6B). In contrast, the increase in screw head diameter resulted in a decrease in the abutment stress from 264.15 MPa to 252.07 MPa and 226.16 MPa, respectively (Fig. 6B).

For screw length, no clear relationship was observed between the maximum von Mises equivalent stress of the implant, the abutment, and the abutment screw (Fig. 6C). Additionally, it was not evident that increasing L values from 4 mm to 5 mm and 6 mm had any distinct effect on the natural frequencies of the model (Fig. 6C). These observations were corroborated by statistical tests, which reported that screw length had no significant impact on these measured parameters (*P*>.05) (Table 5).

DISCUSSION

The Kruskal-Wallis analysis test partially supported the rejection of the null hypothesis. The θ significantly affected implant stress, total deformation, and natural frequency (*P*<.001), whereas no significant impact was detected on abutment screw stress (*P*=.799) or abutment stress (*P*=.852). Additionally, the D significantly influenced abutment screw stress (*P*=.010) and abutment stress (*P*=.002) but had no significant effect on implant stress (*P*=.952), total deformation (*P*=.336), or natural frequency (*P*=.276). Lastly, the findings indicated that L had no significant effect on any of the measured variables (*P*>.05). Furthermore, the Dunn test results in Table 6, which provide pairwise comparisons, further supported the partial rejection of the null hypothesis for specific groups and variables.

Optimum preload force should generate stresses in the range of 60% and 75% of the yield strength of the abutment screw material.[41] These stresses can be controlled by either increasing the coefficient of friction or decreasing the tightening torque to keep the stresses within the optimal range, which in this study should be between 516 MPa and 645 MPa. The maximum von Mises stress in all implant components was mostly below the yield strength of the implant material, except for implant stress in some models, which exceeded the yield strength of the implant material when the θ was 45 degrees, causing plastic deformation. The abutment screw stress in all models exceeded the range of stress caused by optimum preload; however, the stresses were still below the yield strength. However, whether the preload was optimum or not, was not important in this study because the aim was to evaluate and compare between models numerically based on the existing results.

In relation to the findings of this research, the natural frequency of the model decreased significantly as the θ increased (Fig. 6A), indicating a decrease in the stability of implant components based on the assumption that higher natural frequencies would correlate with greater stability. This assumption stems from the understanding that when a model is at resonance, it exhibits maximum displacement, implying that models with higher natural frequencies are more stable. The decrease in stability could be attributed to the reduced contact surface area between the abutment and the implant as the θ decreased. Additionally, it was assumed that as the stability of a model decreases, the likelihood of screw loosening increases, leading to the interchangeability of model stability and screw loosening.

Modal analysis results include 6 types of vibrational modes in the FE model under free vibrations. These modes represent the normal modes of vibration for the model: asymmetric, symmetric, wagging, twisting, scissoring, and

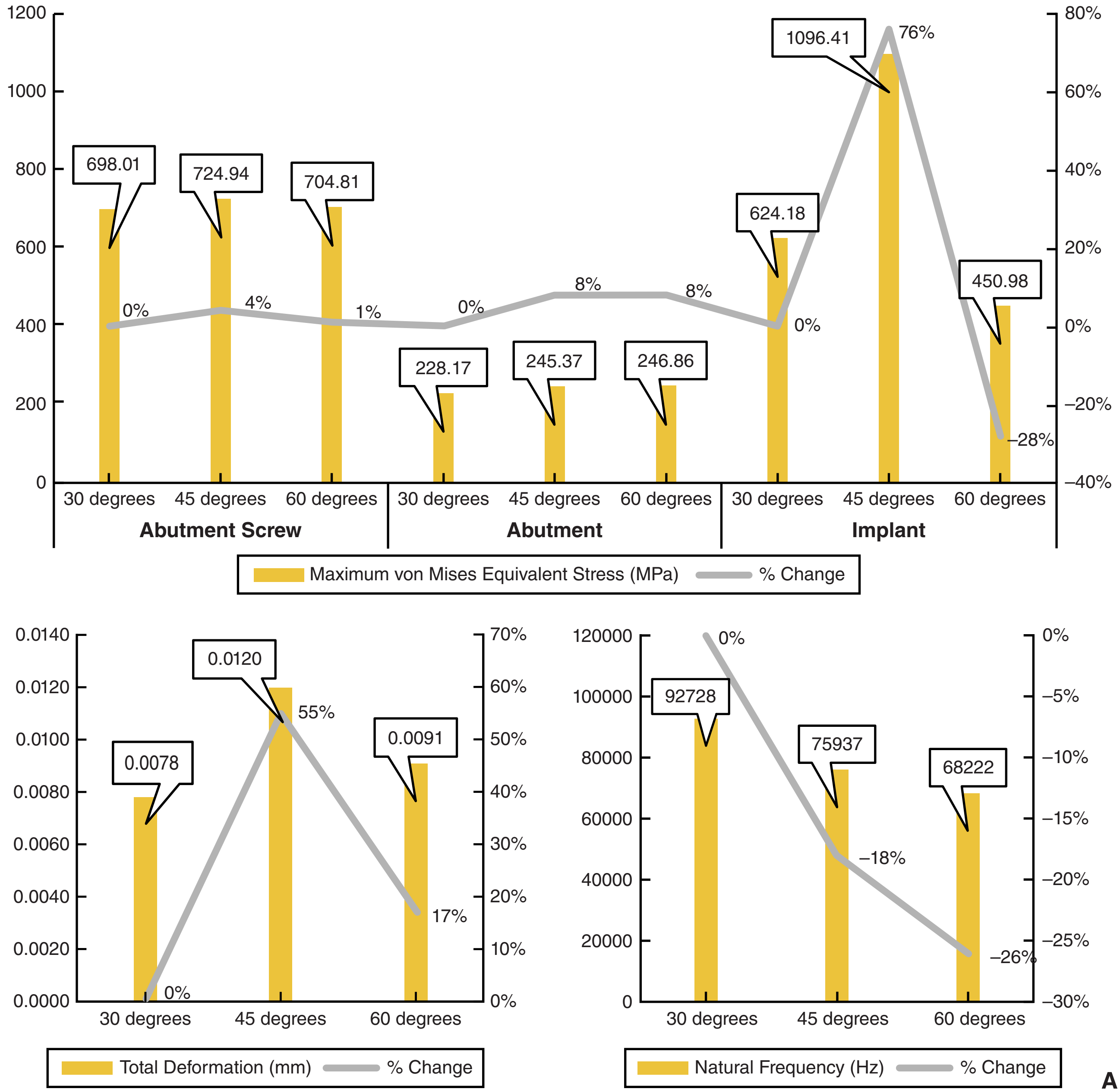

Figure 6. A-C, Main effect of abutment implant angle (θ), abutment screw head diameter (D), and abutment screw length (L) at each level of maximum stresses of implant components, total deformation, and natural frequency for all models.

rocking. The main effect of the natural frequencies of the other 5 modes was inversely proportional to the increase in the θ and directly proportional to the increase in the D, as in mode 1. Therefore, the natural frequencies in all models were presented and compared by using the first mode only to avoid excessive results and plots.

The L had no clear effect on the loosening of the abutment screw, consistent with other studies,[9,10] but not with a study[8] that recommended a long screw with more threads to increase screw retention. The only difference between the models used was the design, whereas the material properties, load and boundary conditions, and contact definitions were the same. Table 4 shows that the difference in obtained stress values between the different screw lengths was small and not statistically significant, indicating that screw length has minimal effect on von Mises stress. Figure 7 demonstrates that the intersection point between the

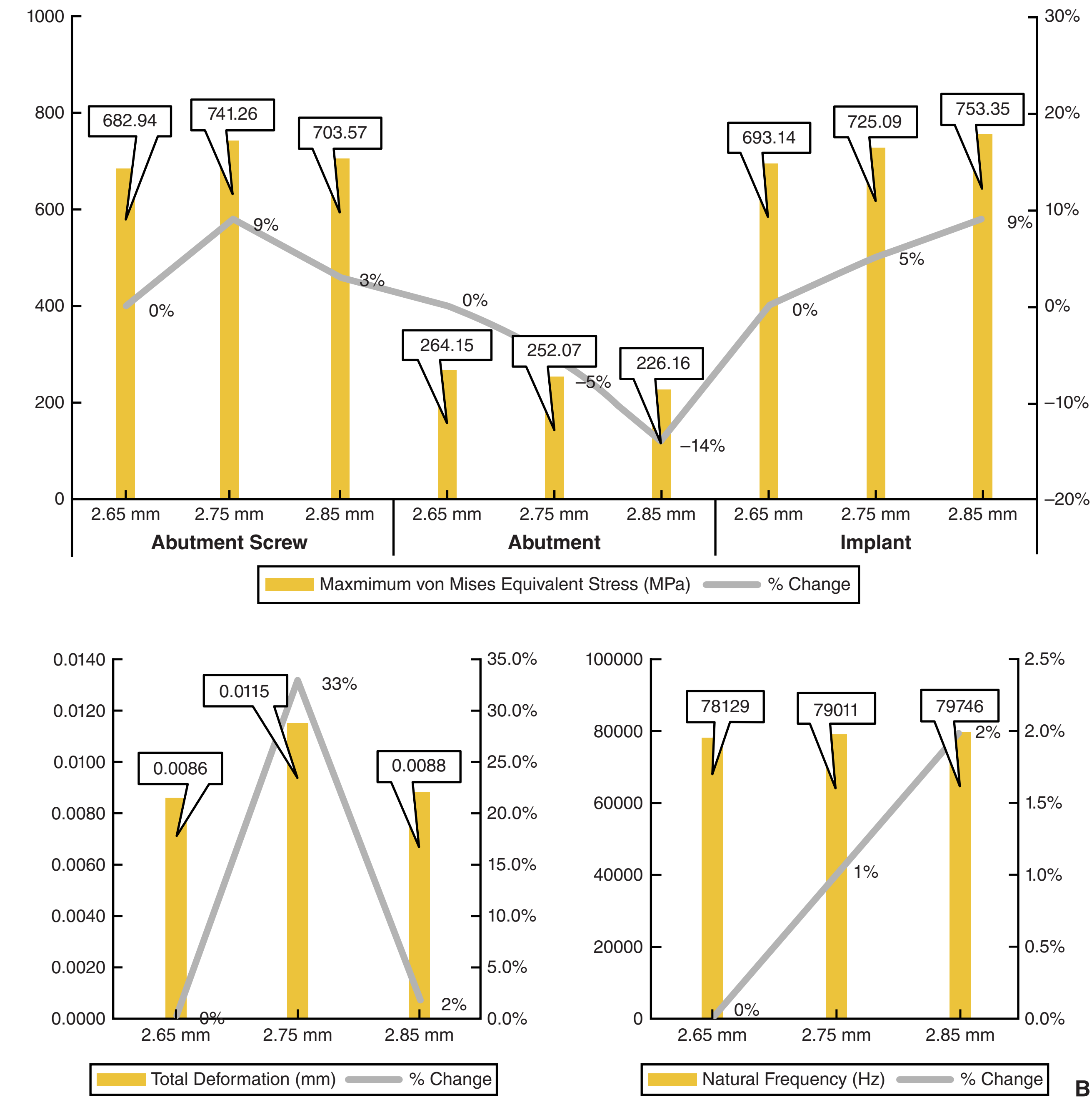

Figure 6. (*continued*)

screw thread and thread slot varied when the θ was changed. This intersection point is crucial because the maximum stress of the abutment screw is located in this region, as shown in Figure 5C. Overall, the absence of this relationship can be attributed to the location of the intersection point between the screw thread and the thread slot.

Limitations of this study included simplifications such as modeling the implant without external threads and not considering the simulation of cortical and cancellous bones around the implant in the FE model. However, these simplifications should not impact the comparative results of the investigated parameters. It was assumed that the implant's external threads had no effect on screw

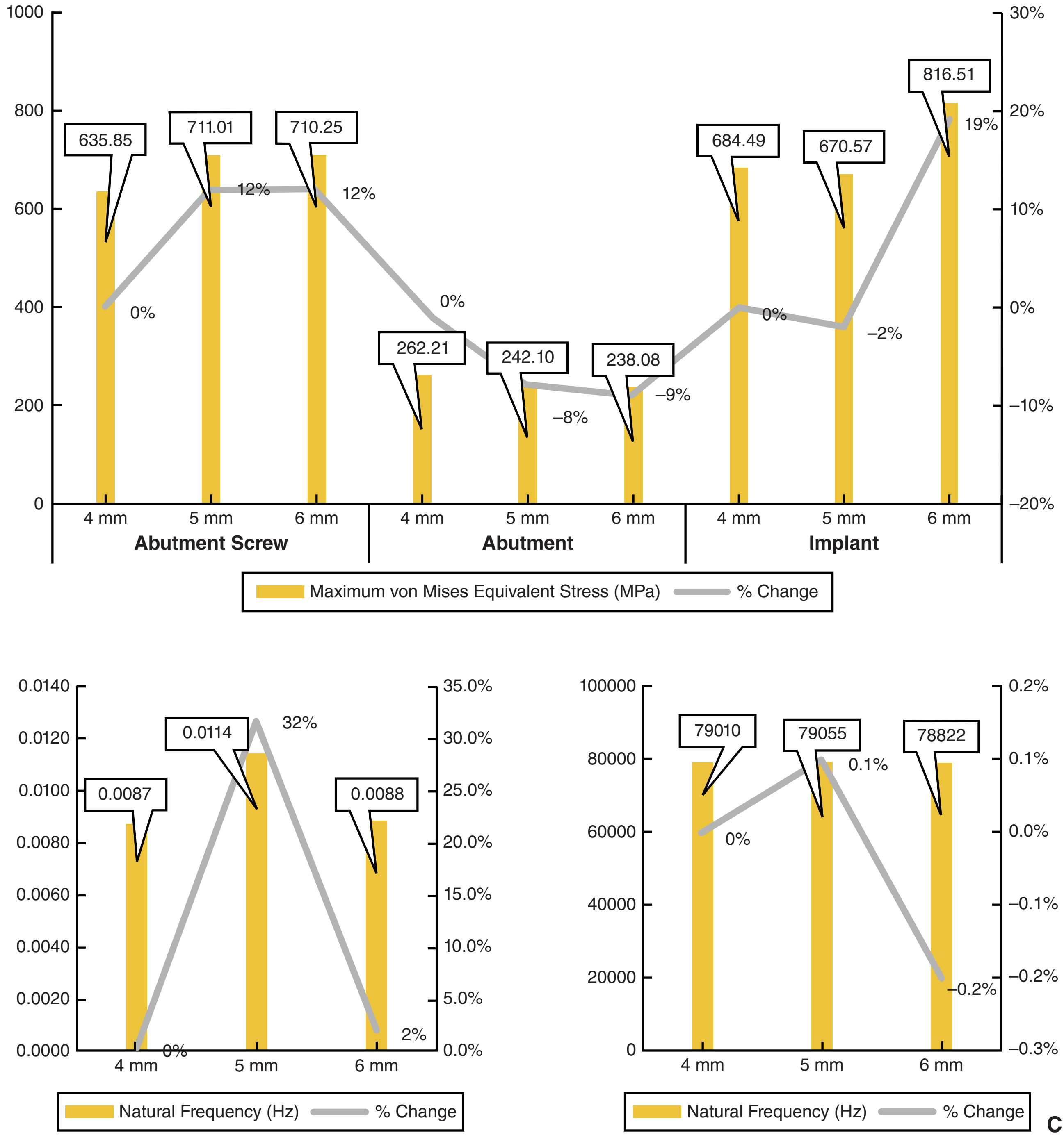

Figure 6. (*continued*)

loosening, and whereas bone may absorb stresses transferred from the implant, affecting the stress values of dental implant components, this aspect was not within the scope of this study. Despite these simplifications, the abutment screw was modeled to accurately represent its real-life counterpart. Therefore, the virtual representation of the abutment screw used in the study considered the physical properties (elastic modulus, yield strength, and Poisson ratio) and geometries (shape, size, and dimensions) of the screw's threads, allowing for a more realistic simulation of the behavior and performance of the actual abutment screw. Further research might be required to fully understand the role of the L in the mechanical stability of dental implants.

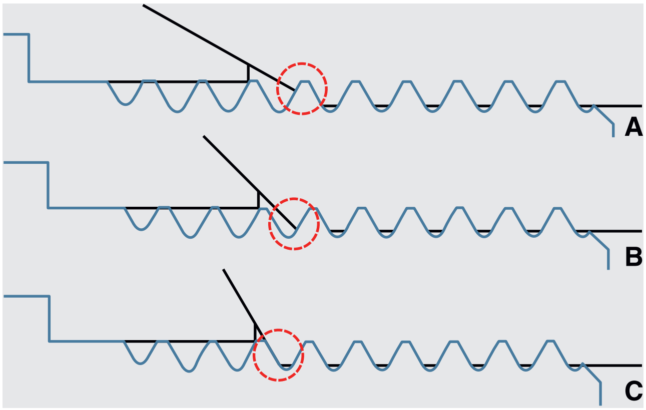

Figure 7. Variation in intersection point between screw thread and screw slot at different abutment implant angles. A, 30 degrees. B, 45 degrees. C, 60 degrees.

CONCLUSIONS

Based on the findings of this 3D FEA study, the following conclusions were drawn:

1. The θ and the D significantly affected the stresses of dental implant components, total deformation, and natural frequency of dental implants. This, in turn, may influence the mechanical stability of the screw joint and the likelihood of screw loosening in dental implants.
2. The L had no significant effect on the dependent variables studied.

REFERENCES

1. Cho SC, Small PN, Elian N, Tarnow D. Screw loosening for standard and wide diameter implants in partially edentulous cases: 3-to 7-year longitudinal data. *Implant Dent*. 2004;13:245–250.
2. Lee KY, Shin KS, Jung JH, Cho HW, Kwon KH, Kim YL. Clinical study on screw loosening in dental implant prostheses: A 6-year retrospective study. *J Korean Assoc Oral Maxillofac Surg*. 2020;46:133.
3. Kreissl ME, Gerds T, Muche R, Heydecke G, Strub JR. Technical complications of implant-supported fixed partial dentures in partially edentulous cases after an average observation period of 5 years. *Clin Oral Implants Res*. 2007;18:720–726.
4. Jemt T, Laney WR, Harris D, et al. Osseointegrated implants for single tooth replacement: A 1-year report from a multicenter prospective study. *Int J Oral Maxillofac Implants*. 1991;6:29–36.
5. Brägger U, Aeschlimann S, Bürgin W, Hämmerle CH, Lang NP. Biological and technical complications and failures with fixed partial dentures (FPD) on implants and teeth after four to five years of function. *Clin Oral Implants Res*. 2001;12:26–34.
6. Pjetursson BE, Tan K, Lang NP, Brägger U, Egger M, Zwahlen M. A systematic review of the survival and complication rates of fixed partial dentures (FPDs) after an observation period of at least 5 years: I. Implant-supported FPDs. *Clin Oral Implants Res*. 2004;15:625–642.
7. Goodacre CJ, Bernal G, Rungcharassaeng K, Kan JY. Clinical complications with implants and implant prostheses. *J Prosthet Dent*. 2003;90:121–132.
8. Kanneganti KC, Vinnakota DN, Pottem SR, Pulagam M. Comparative effect of implant-abutment connections, abutment angulations, and screw lengths on preloaded abutment screw using three-dimensional finite element analysis: An in vitro study. *J Indian Prosthodont Soc*. 2018;18:161–167.
9. Lee JH, Cha HS. Screw loosening and changes in removal torque relative to abutment screw length in a dental implant with external abutment connection after oblique cyclic loading. *J Adv Prosthodont*. 2018;10:415–421.
10. Yeo IS, Lee JH, Kang TJ, et al. The effect of abutment screw length on screw loosening in dental implants with external abutment connection after thermocycling. *Int J Oral Maxillofac Implants*. 2014;29:59–62.
11. Londhe SM, Gowda EM, Mandlik VB, Shashidhar MP. Factors associated with abutment screw loosening in single implant supported crowns: A cross-sectional study. *Med J Armed Forces India*. 2020;76:37–40.
12. Koosha S, Toraji S, Mostafavi AS. Effect of fluid contamination on the reverse torque values of abutment screws at implant-abutment connections. *J Prosthet Dent*. 2020;123:618–621.
13. Sammour SR, Maamoun El-sheikh M, Aly El-Gendy A. Effect of implant abutment connection designs, and implant diameters on screw loosening before and after cyclic loading: In vitro study. *Dent Mater*. 2019;35:e265–e271.
14. Siadat H, Najafi H, Alikhasi M, Falahi B, Beyabanaki E, Zayeri F. Effect of lateral oblique cyclic loading on microleakage and screw loosening of implants with different connections. *J Dent Res Dent Clin Dent Prospects*. 2018;12:183–189.
15. Khraisat A, Hashimoto A, Nomura S, Miyakawa O. Effect of lateral cyclic loading on abutment screw loosening of an external hexagon implant system. *J Prosthet Dent*. 2004;91:326–334.
16. Siamos G, Winkler S, Boberick KG. The relationship between implant preload and screw loosening on implant-supported prostheses. *J Oral Implantol*. 2002;28:67–73.
17. Lee J, Kim YS, Kim CW, Han JS. Wave analysis of implant screw loosening using an air cylindrical cyclic loading device. *J Prosthet Dent*. 2002;88:402–408.
18. Kim KS, Lim YJ. Axial displacements and removal torque changes of five different implant-abutment connections under static vertical loading. *Materials*. 2020;13:699.
19. Hotinski E, Dudley J. Abutment screw loosening in angulation-correcting implants: An in vitro study. *J Prosthet Dent*. 2019;121:151–155.
20. Ha CY, Lim YJ, Kim MJ, Choi JH. The influence of abutment angulation on screw loosening of implants in the anterior maxilla. *Int J Oral Maxillofac Implants*. 2011;26:45–55.
21. Wu T, Fan H, Ma R, Chen H, Li Z, Yu H. Effect of lubricant on the reliability of dental implant abutment screw joint: An in vitro laboratory and three-dimension finite element analysis. *Mater Sci Eng C Mater Biol Appl*. 2017;75:297–304.
22. Bulaqi HA, Barzegar A, Paknejad M, Safari H. Assessment of preload, remaining torque, and removal torque in abutment screws under different frictional conditions: A finite element analysis. *J Prosthet Dent*. 2019;121:548.e1–548.e7.
23. Korioth TWP, Cardoso AC. Effect of washers on reverse torque displacement of dental implant gold retaining screws. *J Prosthet Dent*. 1999;82:312–316.
24. de Moura MB, Rodrigues RB, Pinto LM, de Araújo CA, Novais VR, Júnior PC. Influence of screw surface treatment on retention of implant-supported fixed partial dentures. *J Oral Implantol*. 2017;43:254–260.
25. Sahin C, Ayyildiz S. Correlation between microleakage and screw loosening at implant-abutment connection. *J Adv Prosthodont*. 2014;6:35–38.
26. Siadat H, Pirmoazen S, Beyabanaki E, Alikhasi M. Does abutment collar length affect abutment screw loosening after cyclic loading? *J Oral Implantol*. 2015;41:346–351.
27. Bulaqi HA, Mashhadi MM, Safari H, Samandari MM, Geramipanah F. Dynamic nature of abutment screw retightening: Finite element study of the effect of retightening on the settling effect. *J Prosthet Dent*. 2015;113:412–419.
28. Farina AP, Spazzin AO, Consani RL, Mesquita MF. Screw joint stability after the application of retorque in implant-supported dentures under simulated masticatory conditions. *J Prosthet Dent*. 2014;111:499–504.
29. Aboyoussef H, Weiner S, Ehrenberg D. Effect of an antirotation resistance form on screw loosening for single implant-supported crowns. *J Prosthet Dent*. 2000;83:450–455.
30. Kofron MD, Carstens M, Fu C, Wen HB. In vitro assessment of connection strength and stability of internal implant-abutment connections. *Clin Biomech*. 2019;65:92–99.
31. Arnetzl GV, Payer M, Falkensammer F, Arnetzl G. Effect of double conical abutment screw on implant preload. *Clin Oral Implants Res*. 2016;27:553–557.
32. Coppedê AR, Faria AC, de Mattos Mda G, Rodrigues RC, Shibli JA, Ribeiro RF. Mechanical comparison of experimental conical-head abutment screws with conventional flat-head abutment screws for external-hex and internal tri-channel implant connections: An in vitro evaluation of loosening torque. *Int J Oral Maxillofac Implants*. 2013;28:e321–e329.
33. Butkevica A, Nathanson D, Pober R, Strating H. Measurements of repeated tightening and loosening torque of seven different implant/abutment connection designs and their modifications: An in vitro study. *J Prosthodont*. 2016;27:153–161.
34. Weiss EI, Kozak D, Gross MD. Effect of repeated closures on opening torque values in seven abutment-implant systems. *J Prosthet Dent*. 2000;84:194–199.
35. Arshad M, Mahgoli H, Payaminia L. Effect of repeated screw joint closing and opening cycles and cyclic loading on abutment screw removal torque and screw thread morphology: Scanning electron microscopy evaluation. *Int J Oral Maxillofac Implants*. 2017;33:31–40.

36. Guzaitis KL, Knoernschild KL, Viana MA. Effect of repeated screw joint closing and opining cycles on implant prosthetic screw reverse torque and implant and screw thread morphology. *J Prosthet Dent*. 2011;106:159–169.
37. Xiao H, Yang Y, Liu Z, Taylor TD. Opinions regarding reuse or replacement of implant prosthesis retaining screws: A systematic review. *Int J Oral Maxillofac Implants*. 2017;32:985–991.
38. Park JM, Baek CH, Heo SJ, et al. An in vitro evaluation of the loosening of different interchangeable abutments in internal-connection-type implants. *Int J Oral Maxillofac Implants*. 2017;32:350–355.
39. Alonso-Pérez R, Bartolomé JF, Ferreiroa A, Salido MP, Pradíes G. Original vs. non-original abutments for screw-retained single implant crowns: An in vitro evaluation of internal fit, mechanical behaviour and screw loosening. *Clin Oral Implants Res*. 2018;29:1230–1238.
40. Kim SK, Koak JY, Heo SJ, Taylor TD, Ryoo S, Lee SY. Screw loosening with interchangeable abutments in internally connected implants after cyclic loading. *Int J Oral Maxillofac Implants*. 2012;27:42–47.
41. Guda T, Ross TA, Lang LA, Millwater HR. Probabilistic analysis of preload in the abutment screw of a dental implant complex. *J Prosthet Dent*. 2008;100:183–193.
42. Farina AP, Spazzin AO, Pantoja JM, Consani RL, Mesquita MF. An in vitro comparison of joint stability of implant-supported fixed prosthetic suprastructures retained with different prosthetic screws and levels of fit under masticatory simulation conditions. *Int J Oral Maxillofac Implants*. 2012;27:833–838.
43. Duncan JP, Nazarova E, Vogiatzi T, Taylor TD. Prosthodontic complications in a prospective clinical trial of single-stage implants at 36 months. *Int J Oral Maxillofac Implants*. 2003;18:561–565.
44. Chen J, Wang L, Yang L, Zhang X, Huang B, Li J. The prosthetic screw loosening of two-implant supported screw-retained fixed dental prostheses in the posterior region: A retrospective evaluation and finite element analysis. *J Biomech*. 2021;122:110423.
45. Kitagawa T, Tanimoto Y, Odaki M, Nemoto K, Aida M. Influence of implant/abutment joint designs on abutment screw loosening in a dental implant system. *J Biomed Mater Res*. 2005;75:457–463.
46. Pournasrollah A, Negahdari R, Gharekhani V, Torab A, Ataei SJ. Investigating the effect of abutment-implant connection type on abutment screw loosening in a dental implant system using finite element method. *J Dent Res Dent Clin Dent Prospects*. 2019;13:289–297.
47. Jörn D, Kohorst P, Besdo S, Rücker M, Stiesch M, Borchers L. Influence of lubricant on screw preload and stresses in a finite element model for a dental implant. *J Prosthet Dent*. 2014;112:340–348.
48. Bulaqi HA, Mashhadi MM, Safari H, Samandari MM, Geramipanah F. Dynamic nature of abutment screw retightening: Finite element study of the effect of retightening on the settling effect. *J Prosthet Dent*. 2015;113:412–419.
49. Chen G, Chen Y, Chen Y, Ji S. Dynamics modeling and experimental modal analysis of bolt loosening for lightning rod. *J Vibroeng*. 2020;22:657–671.
50. Jeng MD, Lin YS, Lin CL. Biomechanical evaluation of the effects of implant neck wall thickness and abutment screw size: A 3D nonlinear finite element analysis. *Appl Sci*. 2020;10:3471.
51. Yao KT, Chen CS, Cheng CK, et al. Optimization of the conical angle design in conical implant–abutment connections: A pilot study based on the finite element method. *J Oral Implantol*. 2018;44:26–35.
52. Eraslan O, İnan Ö. The effect of thread design on stress distribution in a solid screw implant: A 3D finite element analysis. *Clin Oral Investig*. 2010;14:411–416.
53. Djebbar N, Serier B, Bachir Bouiadjra BA. Stress distribution of the variable dynamic loading in the dental implant: A three-dimensional finite element analysis. *J Biomim Biomater Biomed Eng*. 2017;31:44–52.
54. Yodrux A, Yodpijit N, Jongprasithpornt M. Stress and displacement analysis of dental implant threads using three-dimensional finite element analysis. *Appl Sci Eng Prog*. 2019;12:216–222.

Corresponding author:
Dr Abdulrahman Al-sanea
Department of Biomedical Engineering
Kocaeli University
Umuttepe-Kabaoglu, Kocaeli 41380
TURKEY
Email: alsane10@gmail.com.

CRediT authorship contribution statement
Abdulrahman Al-sanea: Conceptualization, Methodology, Software, Resources, Data curation, Verification, Formal analysis, Validation, Investigation, Project administration, Writing - original draft, Visualization. **Serkan Aktas**: Conceptualization, Methodology, Software, Resources, Supervision, Project administration, Review and editing. **Talip Celik**: Conceptualization, Methodology, Resources, Software, Validation, Supervision, Project administration, Review and editing. **Yasin Kisioglu**: Funding acquisition, Supervision, Project administration, Review and editing.

https://doi.org/10.1016/j.prosdent.2023.07.007